Supplemental material to "A High-Throughput Computational Dataset of Halide Perovskite Alloys"

Jiaqi Yang,[1], Panayotis Manganaris,[1], and Arun Mannodi-Kanakkithodi [1, a]

[1]*School of Materials Engineering, Purdue University, West Lafayette, Indiana 47907, USA*
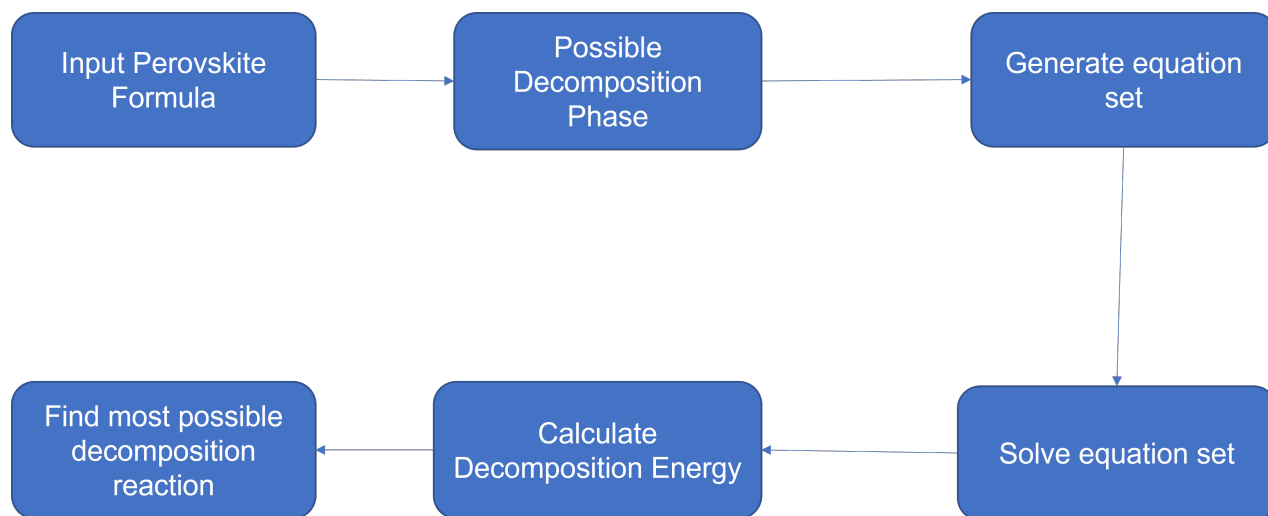
*

Fig. S1 Scheme for determining the perovskite composition energy.

Decomposition Energy Corrections for X-site Mixed Perovskites

Stability with respect to decomposition is one of the most critical properties of halide perovskites. In this research, we define a "decomposition energy" to demonstrate the ease or difficulty of a compound to stay as a perovskite (pseudo-cubic) structure and not decompose to other phases. The formulas used are shown in equations (1) and (2). However, for X-site mixed perovskites, the ratio of decomposed phase is not a unique solution. The fraction of each decomposed phase is varied in a large range, which makes the decomposition energy variable. For instance, $MAPbBr_xI_y$ has 4 possible sets of decomposed phases. The decomposition reaction can be shown using equation (13), and the relationship between the fractions α and β can be calculated by solving equation set (13).

$$MAPbBr_xI_y - > \alpha MABr + (1-\alpha)MAI + \beta PbBr_2 + (1-\beta)PbI_2 \tag{12}$$
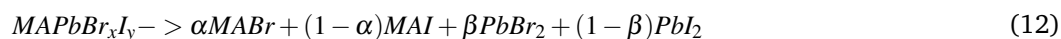
$$\alpha + 2\beta = x$$

$$(1-\alpha) + 2(1-\beta) = y \tag{13}$$

$$\alpha, \beta \in [0,1]$$

To solve this problem, we follow the workflow shown in Fig. S1. To determine which decomposition reaction is most likely, we find the reaction with the highest decomposition energy. Taking $MAPbBr_{1.5}I_{1.5}$ as an example, the PBE decomposition energy is plotted versus the fraction of $PbBr_2$ phase (value of β) in Fig. S2. All other decomposed phases ($MABr$, MAI, PbI_2) can be represented using the fraction of $PbBr_2$. The most likely decomposition reaction turns out to be one that will form $MABr$, $PbBr_2$ and PbI_2; no MAI will be formed. Using this technique, we apply a correction for all

---

* [a]amannodi@purdue.edu
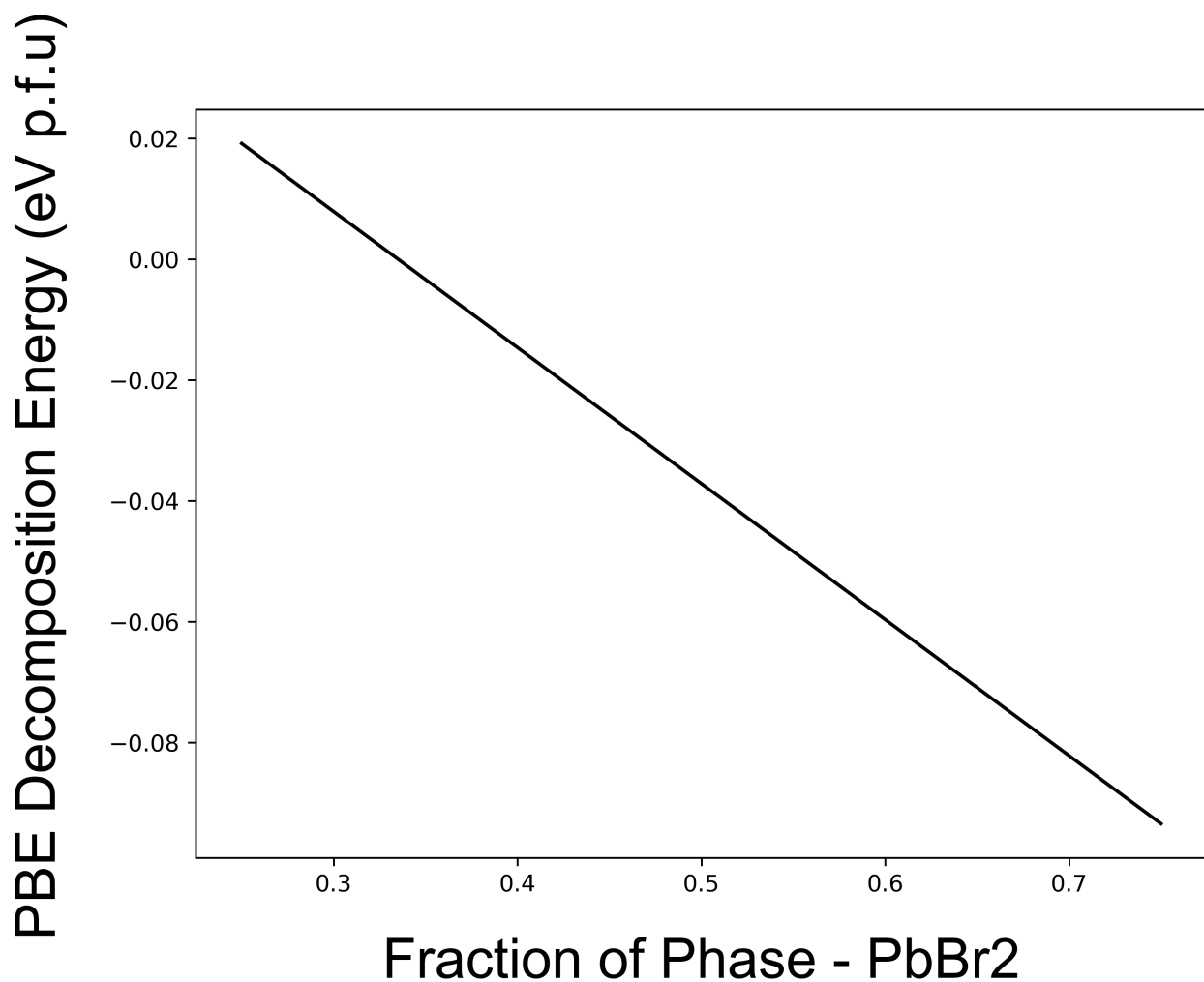
Fig. S2 Decomposition Energy of MAPbBr$_{1.5}$I$_{1.5}$ plotted against the fraction of *PbBr$_2$*.

X-site mixed perovskite in our data set. In the future, a code will be developed and released to fit any complex mixed perovskites and find the decomposition reaction with the highest decomposition energy and probability. The results of these corrections also show us a way to increase the stability of a perovskite: by increasing the amount of decomposed phase in the environment, the decomposition reaction will be pushed to left side (perovskite side) and thus stabilize the bulk material.

| Functional ->	PBE	HSE-rel	HSE-rel+SOC	HSE-PBE+SOC
RMSE of Band Gap (eV)	0.5	1.81	1.41	0.40

Table SI RMSE values for cubic halide perovskites gathered from DFT calculations and experimental measurement.

| Functional	Lattice Constant RMSE (Å)	Lattice Constant Percentage Error
PBE relaxed	0.27	2.21%
HSE relaxed	0.31	3.91%

Table SII RMSE values and error percentage of PBE and HSE lattice constants against experimental values.
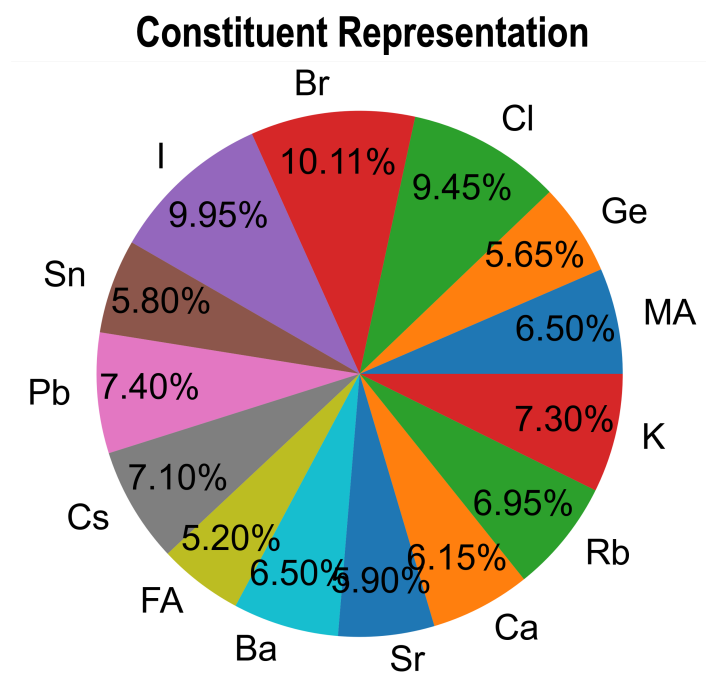
Fig. S3 Pie-chart showing distribution of all molecular and elemental species in the compounds across our computational dataset.
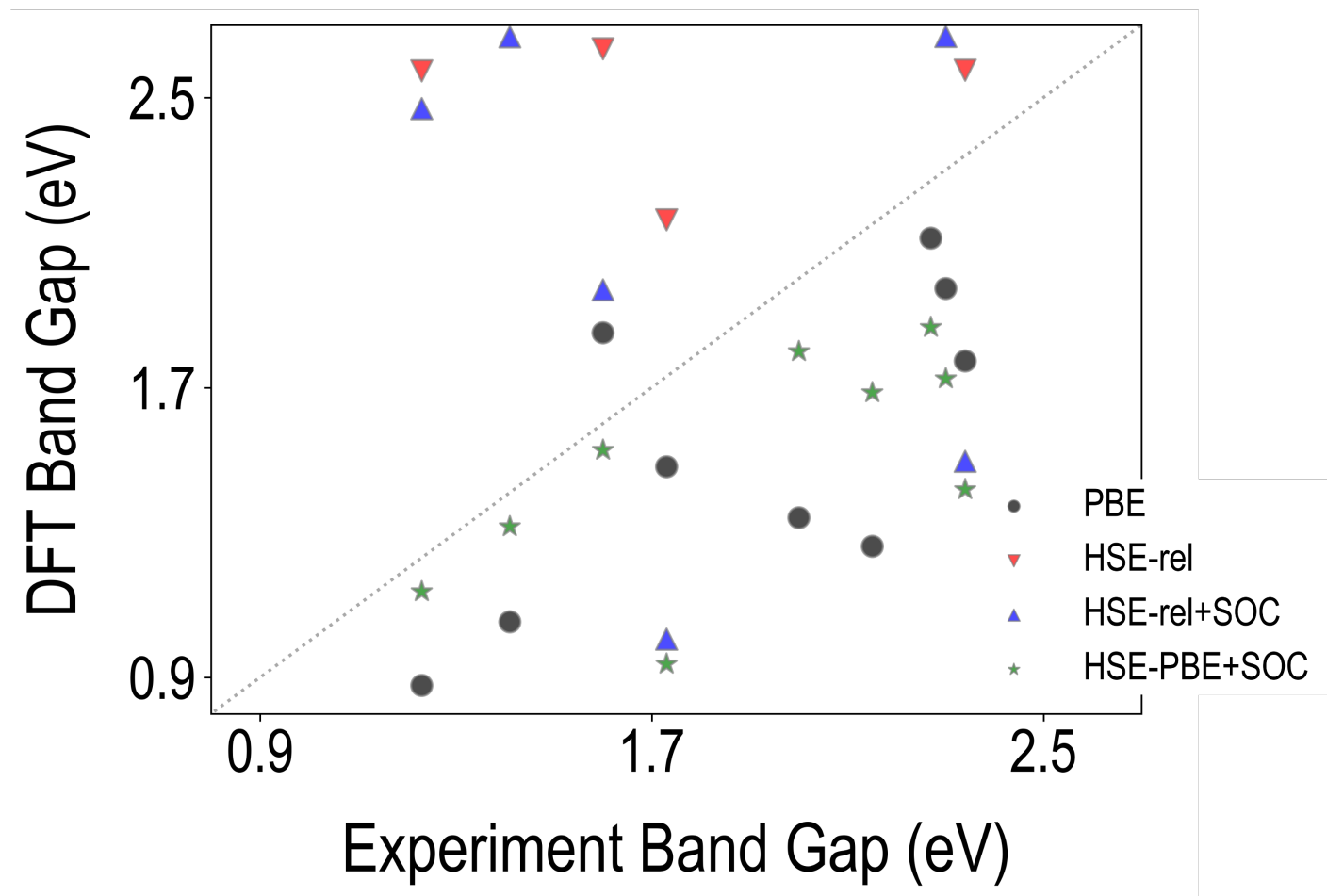
Fig. S4 Comparing DFT computed band gap with experimentally measured values for a selected list of cubic or pseudo-cubic halide perovskites.
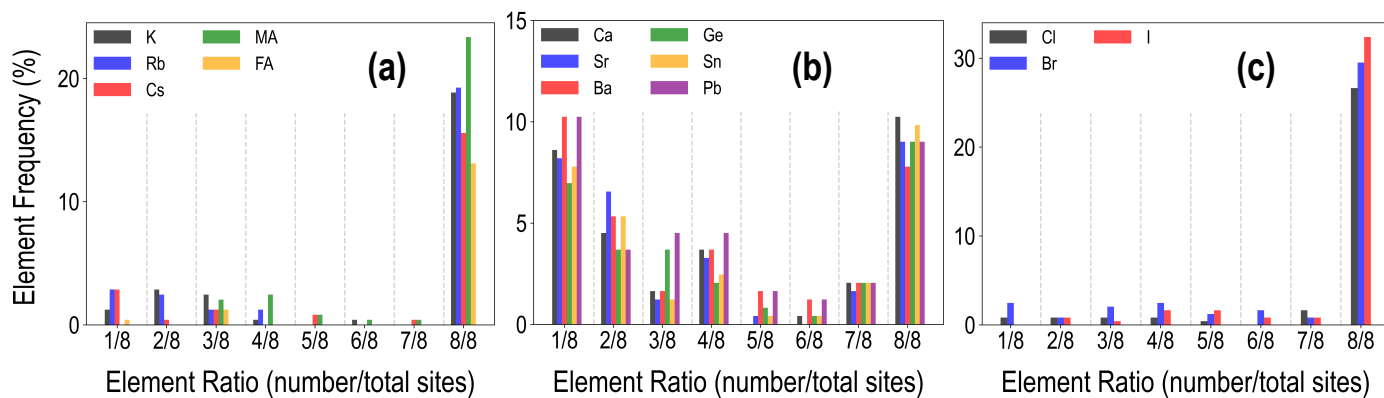
Fig. S5 Distribution of mixing fractions of various species at the A (a), B (b), and X (c) sites across HSE-PBE-SOC dataset.
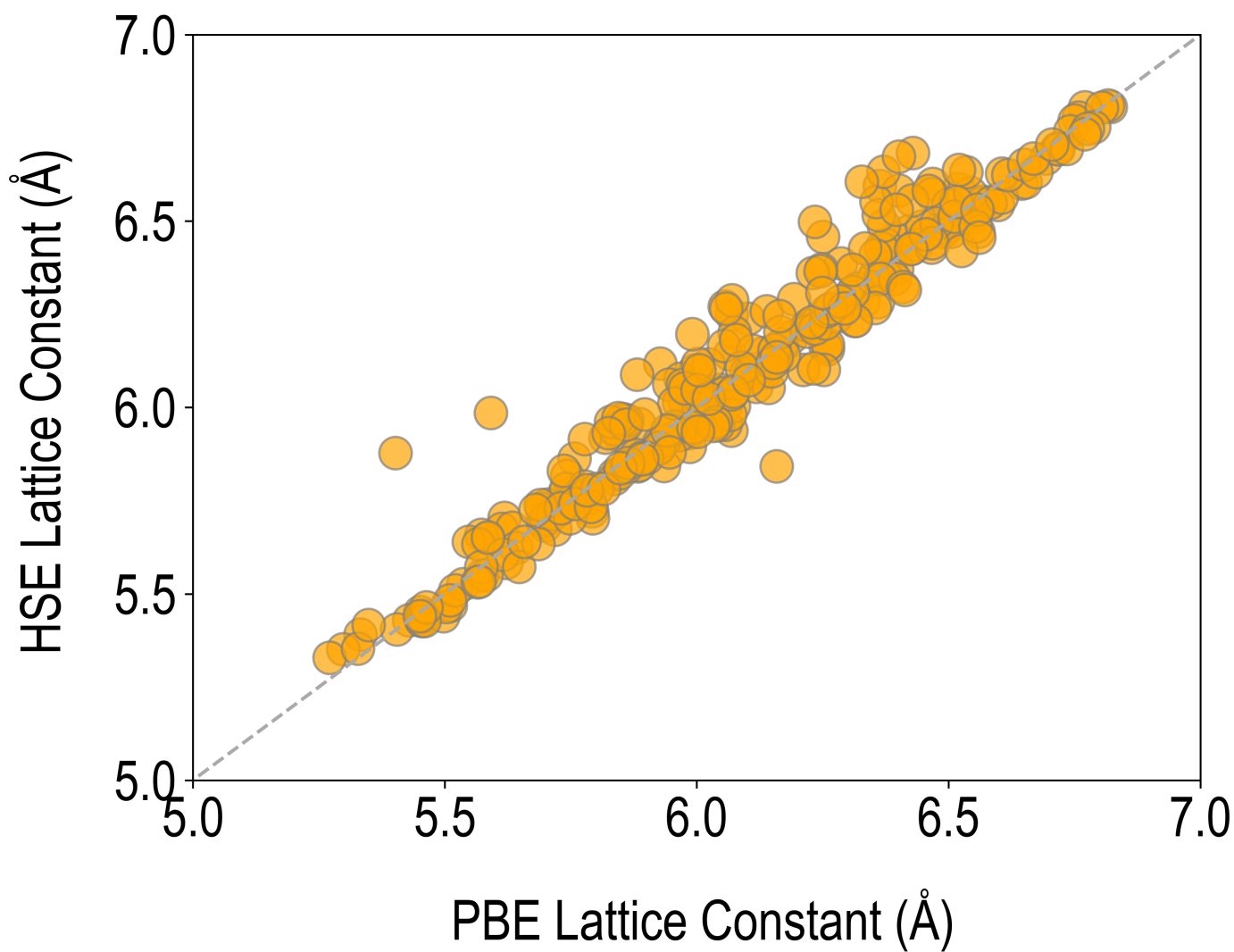
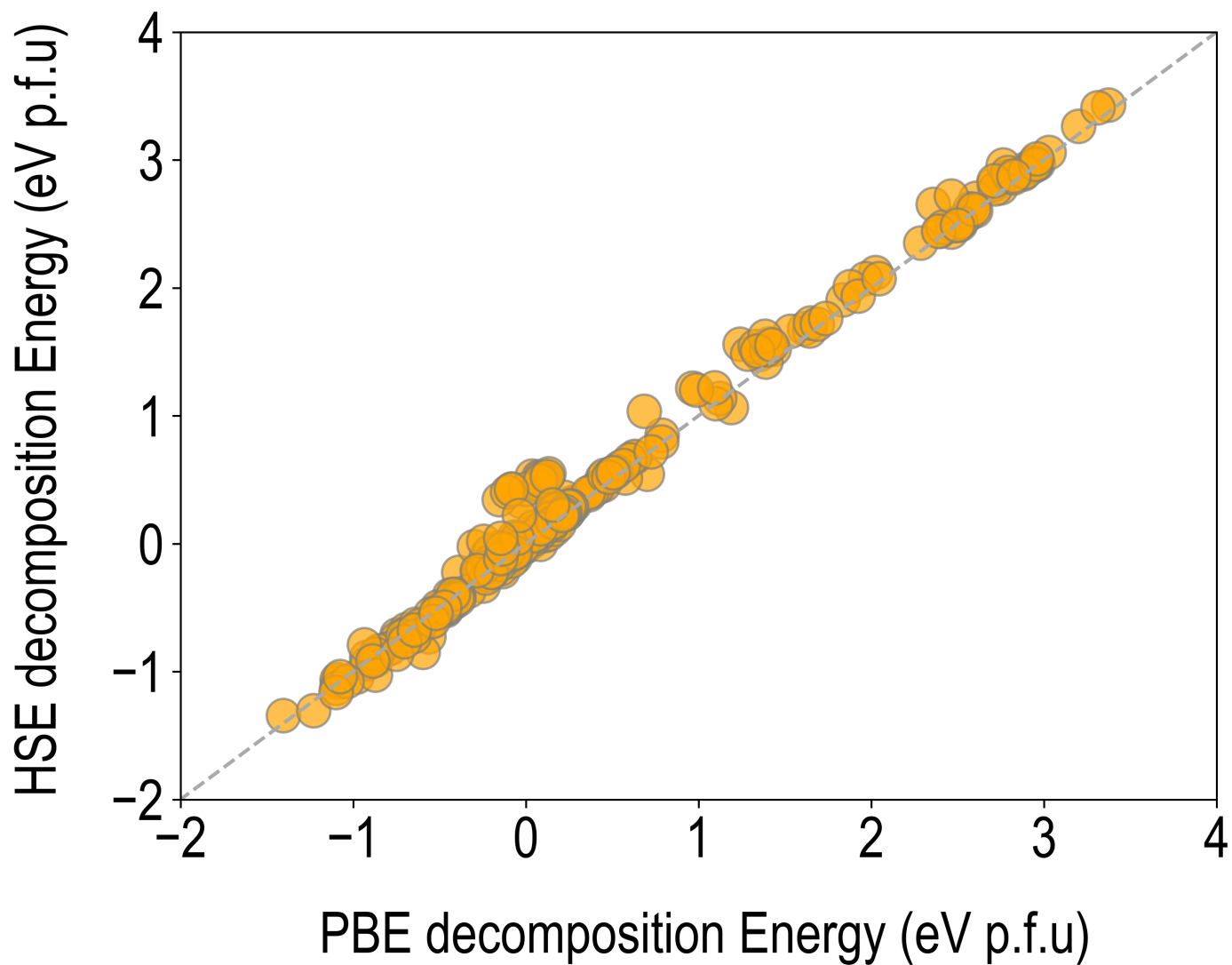**Fig. S6** Comparison between PBE-relaxed and HSE-relaxed pseudo-cubic lattice constants.

Fig. S7 Comparison between PBE-relaxed and HSE-relaxed decomposition energies.
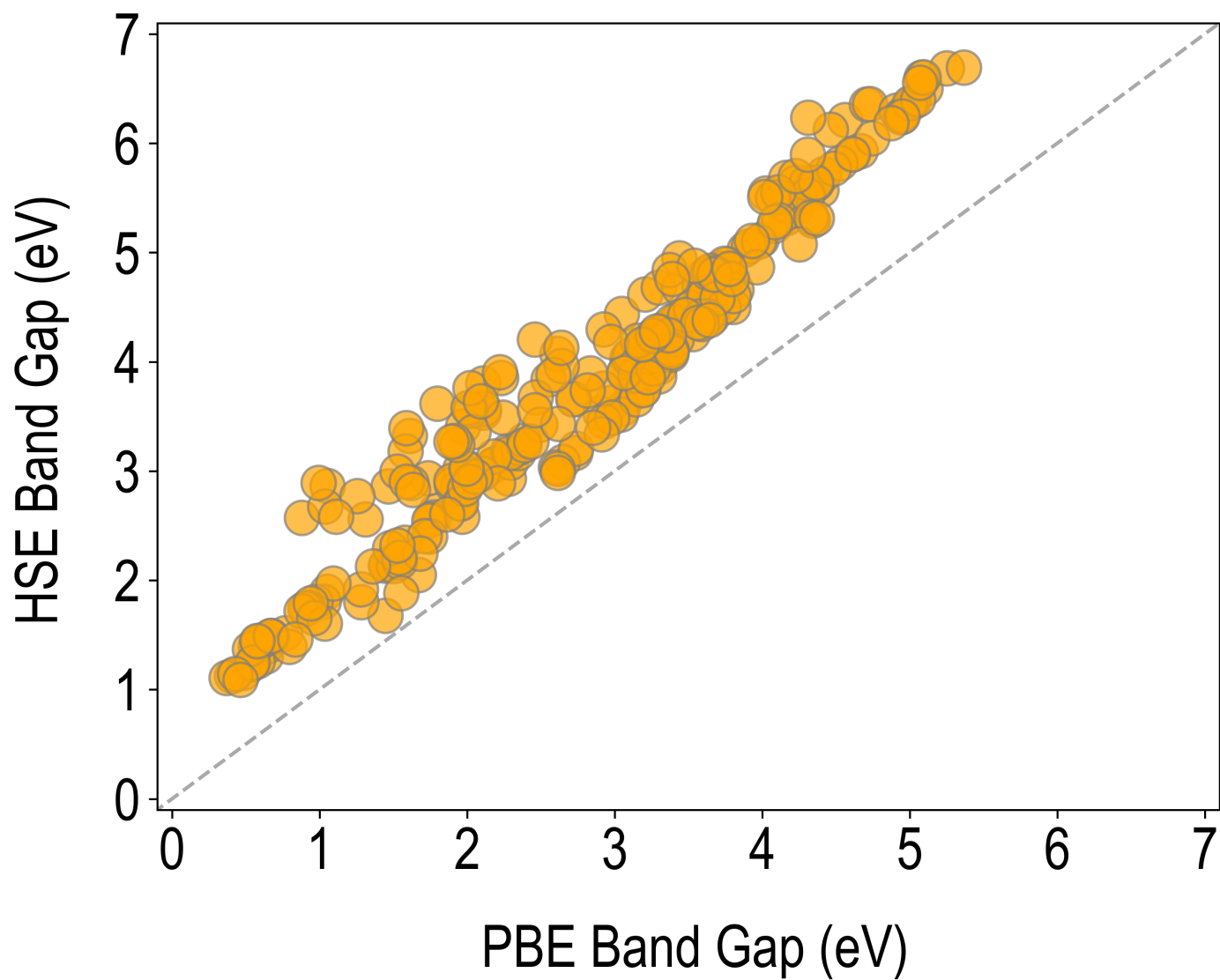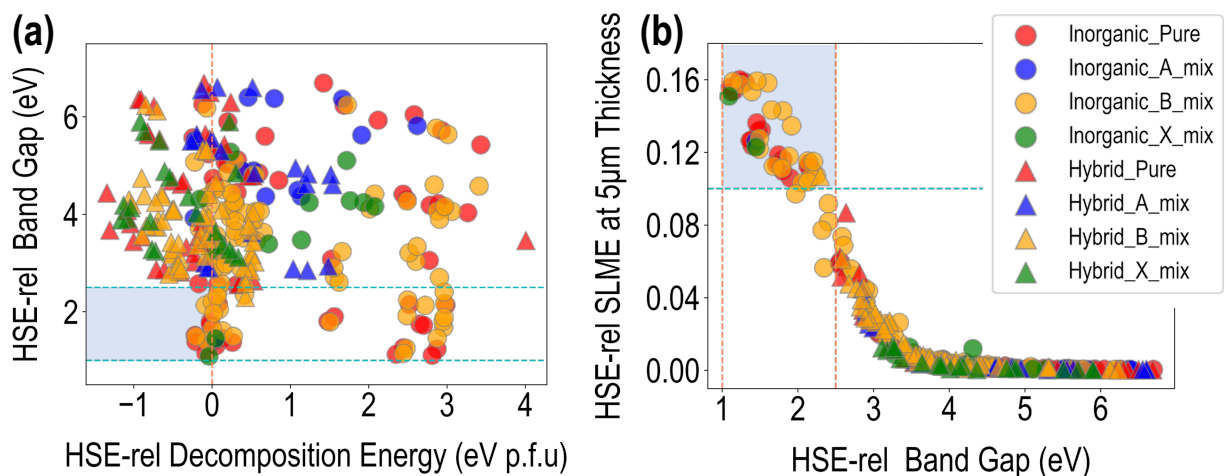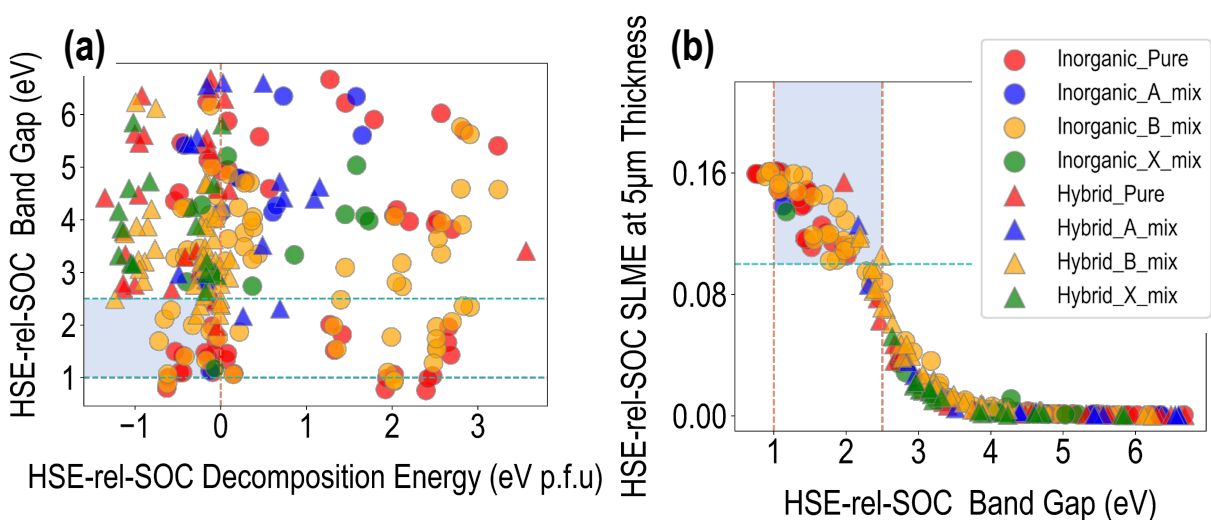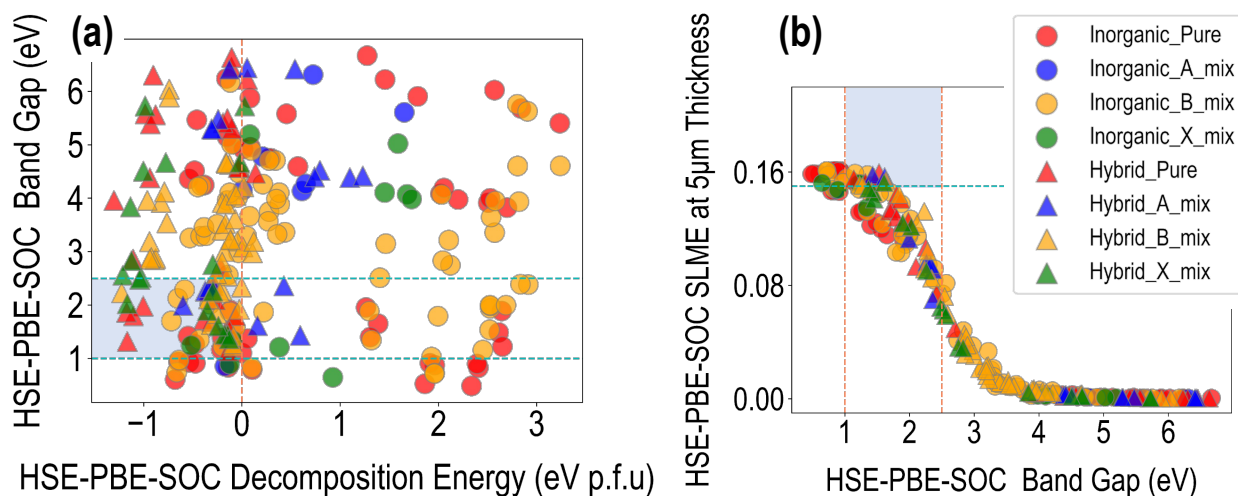
**Fig. S8** Comparison between PBE-relaxed and HSE-relaxed band gaps.

Fig. S9 Visualization of the HSE-relaxed dataset: (a) band gap against decomposition energy, and (b) SLME at 5μm sample thickness against band gap.The shaded regions attempt to capture compounds with negative decomposition energy, band gap between 1 eV and 2.5 eV, and SLME larger than 10%.

Fig. S10 Visualization of the HSE-relaxed with SOC dataset: (a) band gap against decomposition energy, and (b) SLME at 5μm sample thickness against band gap.The shaded regions attempt to capture compounds with negative decomposition energy, band gap between 1 eV and 2.5 eV, and SLME larger than 10%.

Fig. S11 Visualization of the HSE-PBE-SOC dataset: (a) band gap against decomposition energy, and (b) SLME at $5\mu m$ sample thickness against band gap. The shaded regions attempt to capture compounds with negative decomposition energy, band gap between 1 eV and 2.5 eV, and SLME larger than 15%.
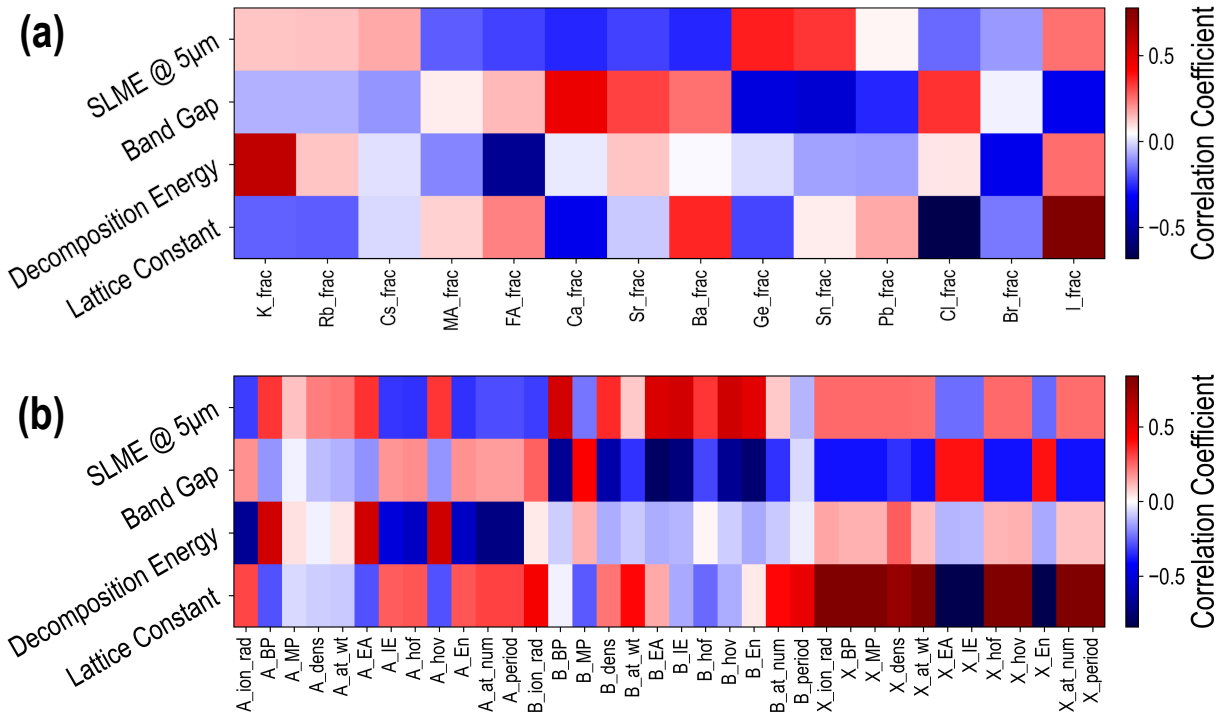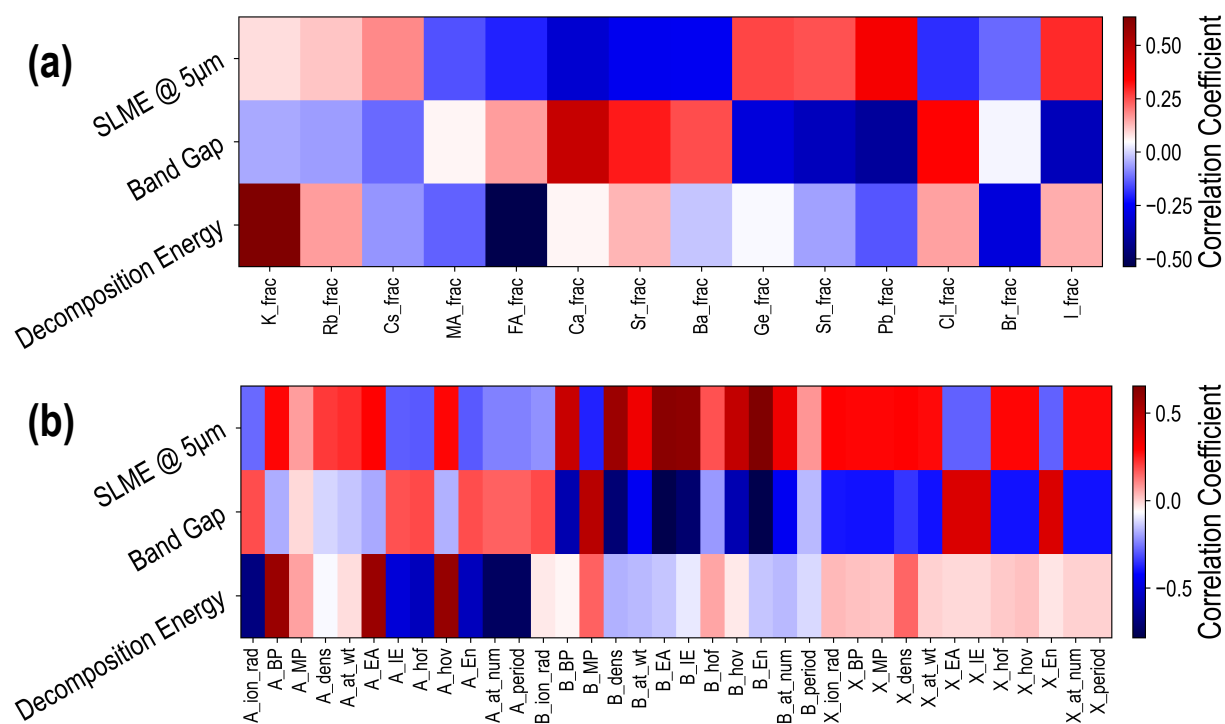

Fig. S12 Pearson coefficients of linear correlation between 4 HSE-relaxed computed properties and (a) 14 compositional descriptors, and (b) 36 elemental property descriptors.

Fig. S13 Pearson coefficients of linear correlation between 3 HSE-rel-SOC computed properties and (a) 14 compositional descriptors, and (b) 36 elemental property descriptors.
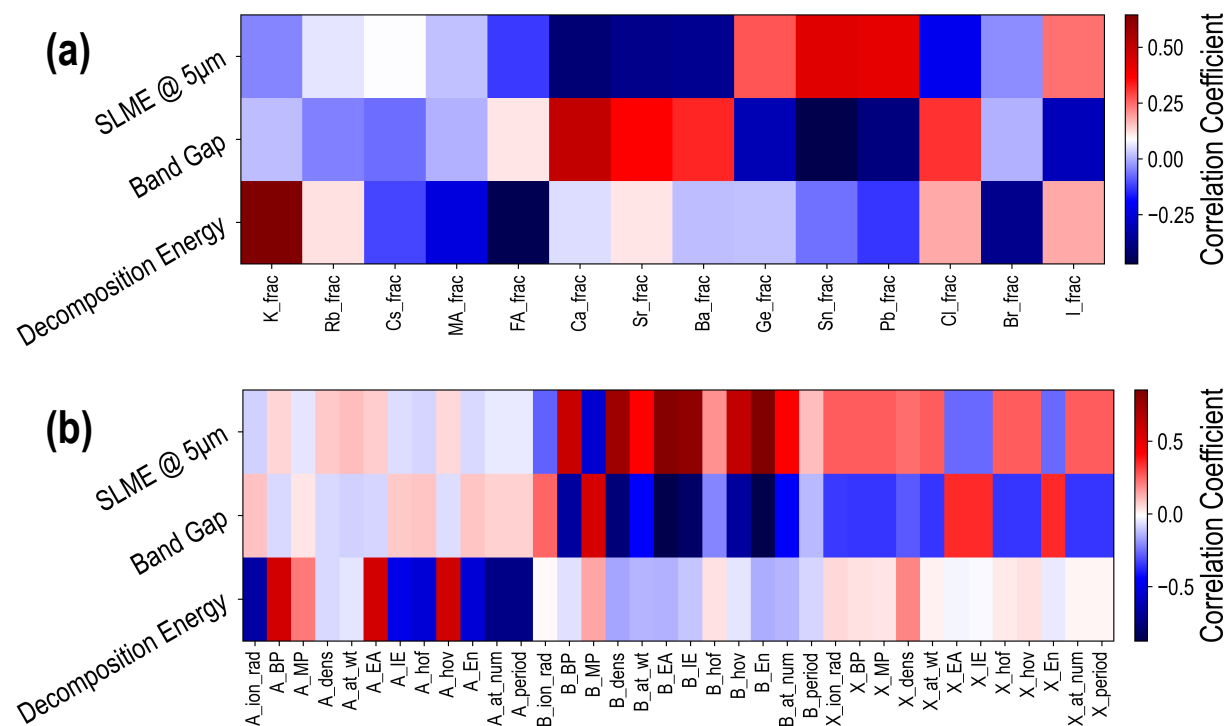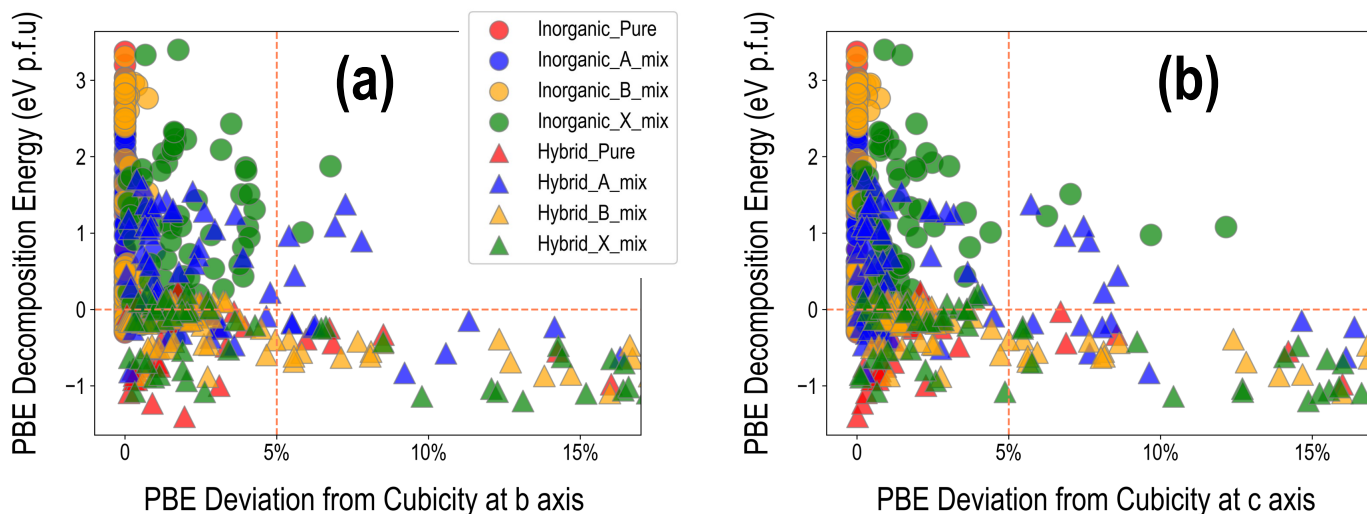

Fig. S14 Pearson coefficients of linear correlation between 3 HSE-PBE-SOC computed properties and (a) 14 compositional descriptors, and (b) 36 elemental property descriptors.

Fig. S15 PBE computed decomposition energy plotted against (a) deviation from cubicity along the b-axis, and (b) deviation from cubicity along the c-axis. The vertical and horizontal dashed lines aim to distinguish between negative and positive decomposition energies and deviation from cubicity > 5% and < 5%.
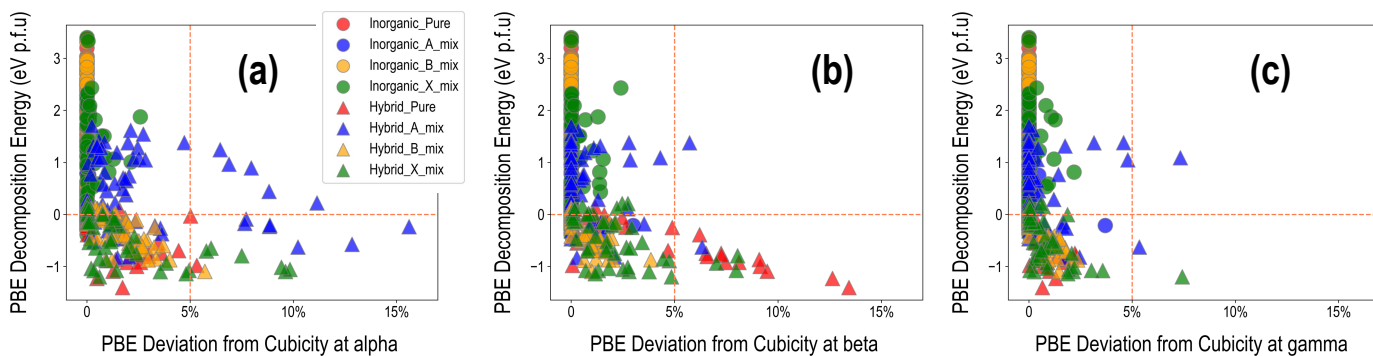
Fig. S16 PBE computed decomposition energy plotted against deviation from cubicity in the (a) angle alpha, (b) angle beta, and (c) angle gamma. The vertical and horizontal dashed lines aim to distinguish between negative and positive decomposition energies and deviation from cubicity > 5% and < 5%.
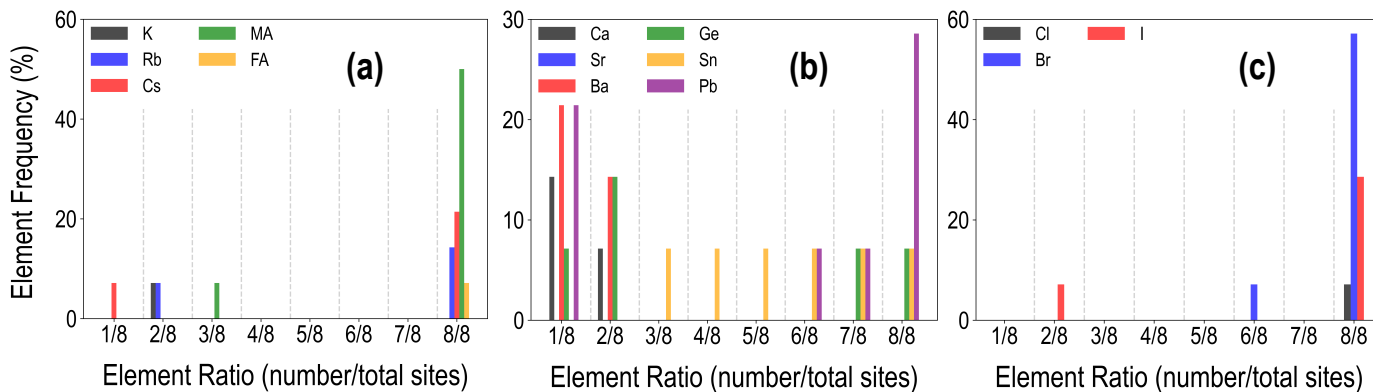
Fig. S17 Distribution of mixing fractions of various species at the A (a), B (b), and X (c) sites across the list of 14 promising compounds selected from the HSE-PBE-SOC dataset.
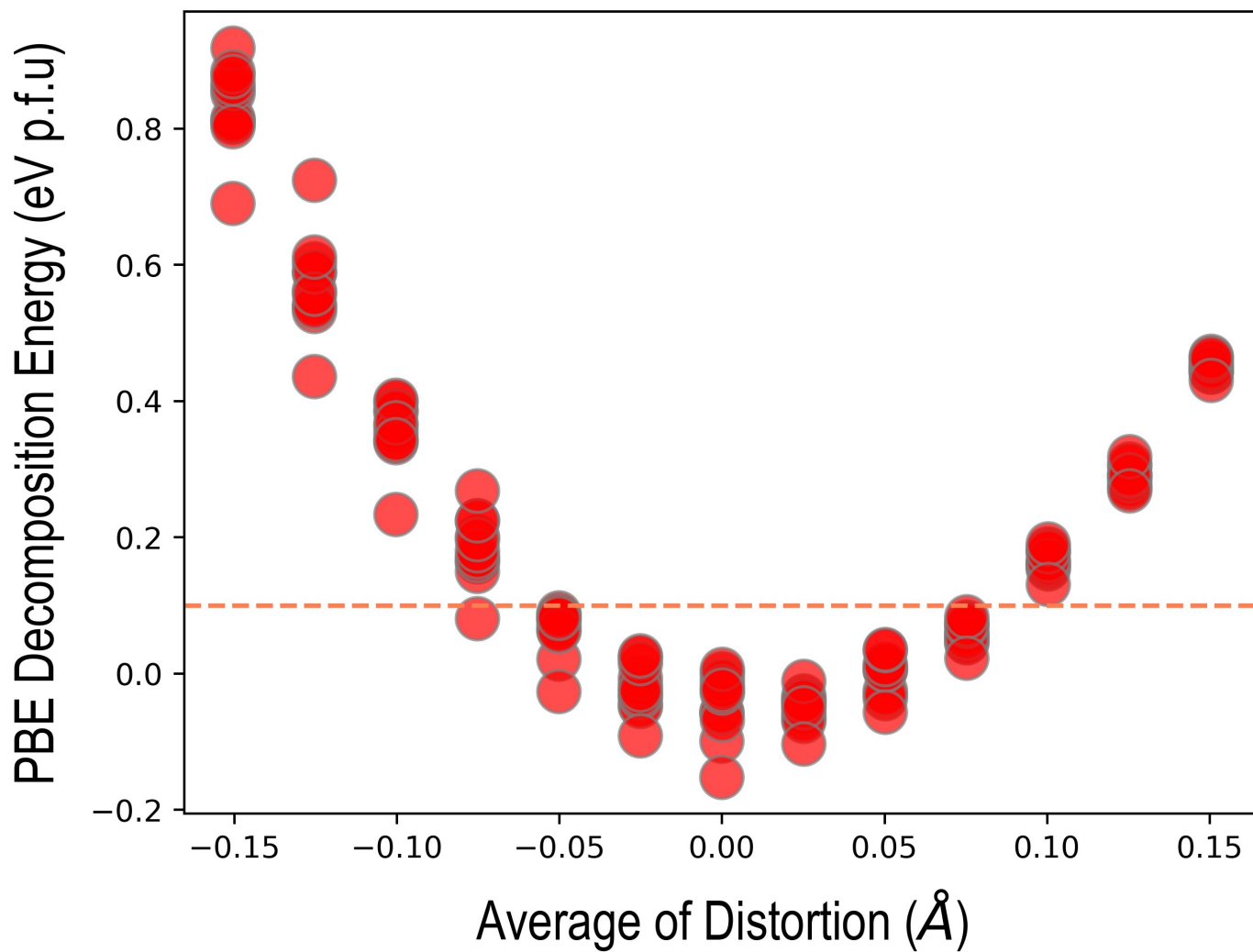
Fig. S18 Decomposition energies computed from PBE for $MAPbBr_3$ compounds with varying amounts of strain and distortion applied to the pseudo-cubic lattice.

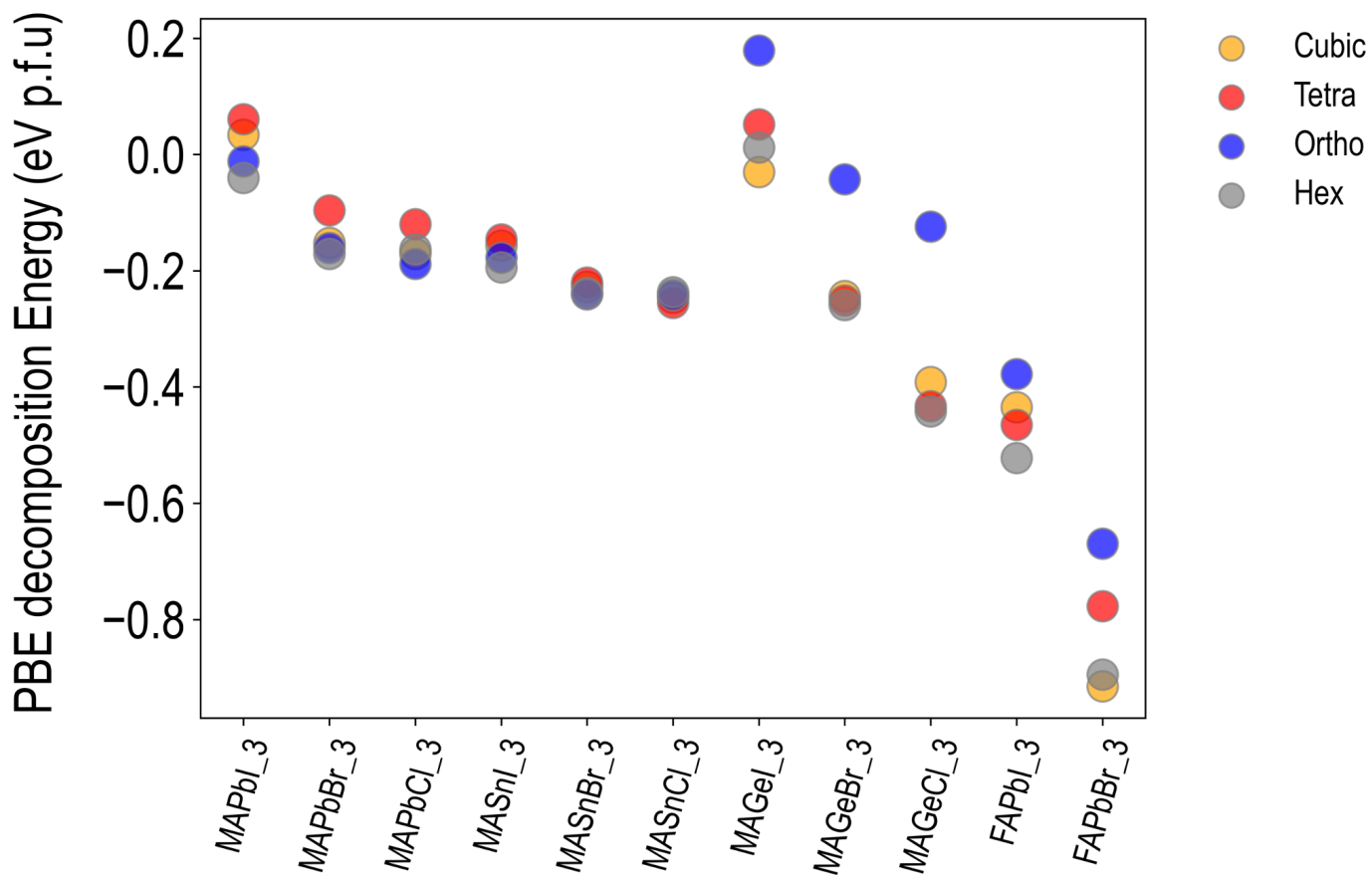**Fig. S19** PBE decomposition energy comparison for selected halide perovskites in 4 different prototypical phases.

Descriptor Label	Descriptor Meaning
K_frac	K fraction over A sites
Rb_frac	Rb fraction over A sites
Cs_frac	Cs fraction over A sites
MA_frac	MA fraction over A sites
FA_frac	FA fraction over A sites
Ca_frac	Ca fraction over B sites
Sr_frac	Sr fraction over B sites
Ba_frac	Ba fraction over B sites
Ge_frac	Ge fraction over B sites
Sn_frac	Sn fraction over B sites
Pb_frac	Pb fraction over B sites
Cl_frac	Cl fraction over X sites
Br_frac	Br fraction over X sites
I_frac	I fraction over X sites
A_ion_rad	Ion radius of A site elements
A_BP	Boiling point of A site elements
A_MP	Melting point of A site elements
A_dens	Density of A site elements
A_at_wt	Atomic weight of A site elements
A_EA	Electron affinity of A site elements
A_IE	Ionization energy of A site elements
A_hof	Heat of formation of A site elements
A_hov	Heat of vaporization of A site elements
A_En	Electronegativity of A site elements
A_at_num	Atomic number of A site elements
A_period	Period number of of A site elements
B_ion_rad	Ion radius of B site elements
B_BP	Boiling point of B site elements
B_MP	Melting point of B site elements
B_dens	Density of B site elements
B_at_wt	Atomic weight of B site elements
B_EA	Electron affinity of B site elements
B_IE	Ionization energy of B site elements
B_hof	Heat of formation of B site elements
B_hov	Heat of vaporization of B site elements
B_En	Electronegativity of B site elements
B_at_num	Atomic number of B site elements
B_period	Period number of of B site elements
X_ion_rad	Ion radius of X site elements
X_BP	Boiling point of X site elements
X_MP	Melting point of X site elements
X_dens	Density of X site elements
X_at_wt	Atomic weight of X site elements
X_EA	Electron affinity of X site elements
X_IE	Ionization energy of X site elements
X_hof	Heat of formation of X site elements
X_hov	Heat of vaporization of X site elements
X_En	Electronegativity of X site elements
X_at_num	Atomic number of X site elements
X_period	Period number of of X site elements

Table SIII Expansion of each compositional and elemental property descriptor label used in this work.

Formula	PBE Band Gap (eV)	PBE Decomposition Energy (eV p.f.u.)	SLME at 5um thickness
$MAGeBr_3$	1.61	-0.25	20.36%
$MASnCl_3$	1.58	-0.25	16.53%
$MASnBr_3$	1.26	-0.23	19.81%
$MAPbBr_3$	1.97	-0.15	11.61%
$CsPbBr_3$	1.77	-0.17	15.35%
$FAPbI_3$	1.94	-0.44	18.64%
$K_{0.125}FA_{0.875}SnBr_3$	1.59	-0.83	18.66%
$K_{0.25}Rb_{0.25}Cs_{0.125}MA_{0.375}PbBr_3$	2.11	-0.07	10.26%
$Rb_{0.375}Cs_{0.25}MA_{0.375}PbBr_3$	2.03	-0.08	12.24%
$FABa_{0.125}Pb_{0.875}I_3$	2.10	-0.42	14.94%
$FABa_{0.25}Pb_{0.75}I_3$	2.35	-0.46	12.03%
$FABa_{0.375}Pb_{0.625}I_3$	2.29	-0.46	11.73%
$CsCa_{0.125}Ba_{0.125}Ge_{0.25}Sn_{0.5}Br_3$	1.50	-0.10	21.85%
$FABa_{0.125}Ge_{0.25}Sn_{0.125}Pb_{0.5}I_3$	1.63	-0.44	18.98%
$MACa_{0.125}Sn_{0.75}Pb_{0.125}I_3$	1.04	-0.08	21.99%
$MABa_{0.25}Ge_{0.125}Sn_{0.625}I_3$	1.48	0.000	22.13%
$MACa_{0.125}Sn_{0.5}Pb_{0.375}Cl_3$	2.01	-0.21	12.34%
$RbCa_{0.25}Ge_{0.25}Sn_{0.375}Pb_{0.125}Br_3$	1.54	-0.01	22.17%
$FABa_{0.125}Ge_{0.125}Sn_{0.75}I_3$	1.26	-0.55	21.85%
$MACa_{0.125}Ge_{0.375}Sn_{0.5}Cl_3$	2.04	-0.25	13.14%
$MABa_{0.125}Pb_{0.875}Br_3$	2.24	-0.12	11.21%
$RbGe_{0.875}Pb_{0.125}Cl_3$	1.09	-0.24	18.15%
$FACa_{0.125}Pb_{0.875}I_3$	1.99	-0.42	17.12%
$MABa_{0.125}Sn_{0.875}I_3$	1.11	-0.08	23.15%
$MACa_{0.125}Pb_{0.875}Br_3$	2.14	-0.13	11.13%
$MASr_{0.125}Pb_{0.875}Br_3$	2.17	-0.13	10.99%
$MAGe_{0.125}Pb_{0.875}Br_3$	2.08	-0.16	11.73%
$MASn_{0.125}Pb_{0.875}Br_3$	1.80	-0.16	14.01%
$CsSnI_{1.875}Br_{1.125}$	2.47	-0.13	10.92%
$CsPbI_{0.75}Br_{2.25}$	2.49	-0.10	16.62%
$CsPbBr_{2.625}Cl_{0.375}$	1.98	-0.16	13.62%
$MAPbI_{2.25}Br_{0.75}$	1.53	-0.79	17.79%

Table SIV Chemical formulas and computed properties for 32 HaPs with desirable properties selected from the PBE dataset.

Formula	Band Gap (eV)	Decomposition Energy (eV p.f.u.)	SLME at 5um thickness
$CsPbI_{0.75}Br_{2.25}$	1.24	-0.52	15.19%
$MACa_{0.125}Sn_{0.75}Pb_{0.125}I_3$	1.23	-0.09	15.12%
$CsPbBr_3$	1.42	-0.55	15.05%
$MABa_{0.125}Sn_{0.875}I_3$	1.41	-0.09	14.68%
$RbCa_{0.25}Ge_{0.25}Sn_{0.375}Pb_{0.125}Br_3$	1.88	-0.12	13.75%
$MAPbBr_3$	1.72	-0.39	13.37%
$FABa_{0.25}Pb_{0.75}I_3$	2.23	-1.22	13.23%
$MASnBr_3$	1.69	-0.31	13.22%
$CsCa_{0.125}Ba_{0.125}Ge_{0.25}Sn_{0.5}Br_3$	2.01	-0.33	12.69%
$MABa_{0.125}Pb_{0.875}Br_3$	2.11	-0.34	12.35%
$RbGe_{0.875}Pb_{0.125}Cl_3$	1.58	-0.07	12.29%
$MABa_{0.25}Ge_{0.125}Sn_{0.625}I_3$	1.91	-0.03	12.08%
$K_{0.25}Rb_{0.25}Cs_{0.125}MA_{0.375}PbBr_3$	1.99	-0.60	11.27%
$MAGeBr_3$	2.25	-0.34	10.67%

Table SV Chemical formulas and computed properties for 14 HaPs with desirable properties selected from the HSE-PBE-SOC dataset.